Atmospheric Pollution Research 6 (2015) 815-823

Atmospheric Pollution Research

www.atmospolres.com

Chemical composition of $PM_{2.5}$ at a high–altitude regional background site over Northeast of Tibet Plateau

Zhuzi Zhao [1,2,3], Junji Cao [1,3], Zhenxing Shen [4], Ru–Jin Huang [5], Tafeng Hu [1], Ping Wang [1], Ting Zhang [1], Suixin Liu [1]

[1] *Key Lab of Aerosol Chemistry & Physics, Institute of Earth Environment, Chinese Academy of Sciences*
[2] *University of Chinese Academy of Sciences*
[3] *SKLLQG, Institute of Earth Environment, Chinese Academy of Sciences*
[4] *Department of Environmental Science and Engineering, Xi'an Jiaotong University, China*
[5] *Laboratory of Atmospheric Chemistry, Paul Scherrer Institute, 5232 Villigen, Switzerland*

ABSTRACT

Aerosol samples were collected from a site near Qinghai Lake (QHL) on the northeastern margin of the Tibetan Plateau (TP) to investigate $PM_{2.5}$ mass levels and chemical composition, especially their seasonal patterns and sources. The $PM_{2.5}$ ranged from 5.7 to 149.7 μg m^{-3}, and it was predominately crustal material (~40% on average). The combined mass of eight water–soluble inorganic ions ranged from 1.0 to 41.5 μg m^{-3}, with the largest contributions from SO_4^{2-}, NO_3^-, and Ca^{2+}. Low abundances of organic carbon (OC, range: 1.0 to 8.2 μg m^{-3}) and elemental carbon (EC, 0.2 to 2.3 μg m^{-3}) were found in QHL. Weak seasonality in the OC/EC ratio (4.5±2.0) indicated simple and stable sources for carbonaceous particles. The water–soluble ions, OC and EC accounted for ~30%, 10% and 2% of the $PM_{2.5}$, respectively. Water–soluble organic carbon (WSOC, range: 0.5 to 4.3 μg m^{-3}) accounted for 47.8% of the OC. Both OC and WSOC were positively correlated with water–soluble K^+ (r=0.70 and 0.73 respectively), an indicator of biomass burning. Higher WSOC and stronger correlations between WSOC and EC in spring and winter compared with summer and autumn are evidence for primary biomass burning aerosols. The concentrations of mass and major compositions were 2–10 times higher than those for some TP or continental background sites but much lower than urban areas. Compared with particles produced from burning yak dung (a presumptive source material), $PM_{2.5}$ had higher SO_4^{2-}/OC ratios. The higher ratios were presumed as a result of fossil fuel combustion. After excluding data for dust storms events, the relative percentages of OM, EC, K^+, NH_4^+, NO_3^- and mineral dust showed little difference among seasons despite different monsoons dominated in four seasons; implying that the $PM_{2.5}$ sources were relatively stable. The results from QHL evidently reflect regional characteristics of the aerosol.

Keywords: *Carbonaceous aerosols, $PM_{2.5}$, chemical composition, Qinghai Lake, Tibet Plateau*

doi: 10.5094/APR.2015.090

Corresponding Author:
Junji Cao
☎ : *+86-88326488*
🖷 : *+86-88320456*
✉ : *jjcao@ieecas.cn*

Article History:
Received: 09 September 2014
Revised: 29 January 2015
Accepted: 01 March 2015

1. Introduction

Atmospheric aerosols are key components of the Earth's systems because of the important roles they play in terms of air–quality, atmospheric chemistry, visibility, human health, climate, etc. Knowledge of aerosol sources and properties at remote sites is important not only for assessing the effects of pollution transport but also for investigating large–scale aerosol effects on biogeochemical cycles and climate (Ramanathan and Carmichael, 2008; Qu et al., 2009; Xu et al., 2009). The Tibet Plateau (TP), the highest plateau on earth, is a remote region with low population density and few industries. Even so, the TP is known to be affected by pollution, and in recent decades, a rapid increase in aerosol pollution has seriously influenced its climate and ecological environment (Engling et al., 2011; Zhao et al., 2013). Studies of aerosol pollution on the TP are also timely, because the region is particularly vulnerable to climate change (Lau and Kim, 2006; Lau et al., 2010).

Qinghai Lake (QHL, 36°32'~37°15'N, 99°36'~100°47'E, 3 200 m a.s.l.) is a closed–basin and the largest brackish lake in China, and it is situated on the northeastern margin of the TP. Previous studies at QHL have mainly focused on paleoclimate and paleoenvironment, and the information was mostly drawn from studies of sediments and the water chemistry (Jin et al., 2010a; Jin et al., 2010b). Recently, some short–term studies have been conducted in the QHL region, focusing mainly on organic compounds, black carbon and source identification (Li et al., 2013; Wang et al., 2014; Zhang et al., 2014a). The atmospheric environment at QHL is distinguished by strong solar radiation and minimal human activity, and therefore the chemical and physical properties of the aerosol differ from those in low–elevation regions (Li et al., 2013). Indeed, atmospheric monitoring has been conducted for many years at the Mt. Waliguan Observatory (N36°17', E100°54', 3 816 m a.s.l., see the Supporting Material, SM, Figure S1a), a Global Atmosphere Watch baseline station. Nonetheless, long–term comprehensive studies properties of aerosol chemical composition in the region are still needed. Here, we present the results of a one–year study of $PM_{2.5}$, including carbonaceous aerosol, water–soluble inorganic ions, dust–derived and other trace elements in aerosols at QHL. Major objectives for the paper were to provide baseline levels of aerosols for this region and characterize the seasonal variability of these substances.

2. Methodology

2.1. Site description

QHL lies in a transitional zone where the climate is driven by the East Asian and Indian monsoons in summer and by the westerly jet in winter and spring (Jin et al., 2010b). The area is characterized by long, cold, and dry winters; short and humid summers; and strong winds, especially in spring. The seasonal mean temperatures were 0.9, 10.9, 4.5, and –8.7 °C from spring to

winter in sampling period. The mean annual precipitation is approximately 337 mm a^{-1} (1951–2005), and precipitation shows clear seasonality, with more than 65% of it falling in summer.

A 12–m–tall air–sampling tower was erected on Bird Island (N36°58′37″, E99°53′56″), which is located on west–northwestern shore of QHL (see the SM, Figure S1). The area surrounding the site is pristine, with sparse vegetation typical of arid and semiarid grasslands. There are no major industrial sources of pollutants nearby; but there is a small village, which is home to about 1 500 Tibetan natives, ~50 km from the sampling site. The villagers use electric power for utilities and lighting, and burn coal and yak dung for cooking and heating. The "heating season" is nominally from October to the following April.

2.2. Aerosol sampling

Two sets of $PM_{2.5}$ samples were collected from an open platform on the top of the air–sampling tower from November 2011 to November 2012: one set was for studies of carbonaceous species and inorganic ions. Those samples were collected on pre–combusted quartz–fiber filters (20×25 cm, Whatman, USA) using a high–volume air sampler (Model TE–6001–2.5–I $PM_{2.5}$ SSI, Tisch Inc., USA), which operated at a flow rate of 1.1 m^3 min^{-1}. The second set of $PM_{2.5}$ samples was used for studies of trace elements, and they were collected on 47 mm diameter Teflon™–membranes (Whatman, USA) from January to November 2012 using a Partisol–Plus Model 2025 Sequential Air Sampler (Rupprecht & Patashnick Co., Inc., USA, 16.7 L min^{-1}). The samples were collected every sixth day starting at 10:00 Beijing Time and each sample was run for 24 h. A total of 56 quartz–fiber and 48 Teflon™ filters were collected. Also, four field blank filters were collected in each season by exposing filters in the samplers for 24 h without drawing air through them. Field filter samples were put into a refrigerator at the tower after sampling, and transported every three months in a portable cooler to laboratory, and then stored at –18 °C prior to analysis. All measured data were corrected for backgrounds from blank filters.

2.3. Collection of fresh aerosol from yak dung burning

A local Tibetan family cooperated in the study, and a Mini_TAS $PM_{2.5}$ sampler (Airmetrics, USA, 5 L min^{-1}) was set up ~1 m downwind of the exhaust outlet of their domestic chimney. Fresh $PM_{2.5}$ particles emitted from household yak dung–burning were collected on a quartz filter, wrapped in aluminum foil, sealed in a plastic bag, and stored together with the ambient samples at –18 °C prior to analysis. Sampling time for fresh yak dung burning sample is four hours; the values of chemical compositions were normalized in μg per filter instead of μg m^{-3} for comparison.

2.4. Sample analysis

Teflon–filters were analyzed gravimetrically for mass concentrations with a Sartorius MC5 electronic microbalance balance with ±1 μg sensitivity (Gottingen, Germany). Prior to weighing, the samples were allowed to equilibrate for 24 h at room temperature (20~23 °C) and relative humidity between 35 and 45%. Each filter was weighed at least three times before and after sampling, and the net mass was obtained by subtracting the difference between the averaged pre– and post–sampling weights. The RSD for weighing of filters before and after sampling were lower than 0.01% and 0.03%, respectively.

The concentrations of eight inorganic ions (Na^+, NH_4^+, K^+, Mg^{2+}, Ca^{2+}, Cl^-, NO_3^- and SO_4^{2-}) were determined with a DX600 ion chromatography (Dionex Inc., USA). Aliquots (~4.33 cm^2) of the quartz sample filters were extracted with 10 mL of ultrapure water. The detailed analysis methods for inorganic ions can be found elsewhere (Zhang et al., 2011; Zhang et al., 2014b). One in 10 extracts was reanalyzed and none of the differences between these replicates exceeded precision intervals. Blank values were also subtracted from sample concentrations.

Subsamples of the aqueous extracts were analyzed for water–soluble organic carbon (WSOC) using a TOC–L CPH Total Carbon Analyzer (Shimadzu Corp., Japan). 25 mL of water–extract is injected into the furnace packed with platinum catalyst at 680 °C. The CO_2 evolved is measured using an NDIR detector to assess total water soluble carbon (TWSC) content. Another aliquot of the solution (100 mL) is acidified with 25% phosphoric acid (25% H_3PO_4, vol/vol) and the evolved CO_2 is interpreted as water soluble inorganic carbon (WSIC). WSOC was obtained by subtracting WSIC from TWSC. The detector response for TWSC and WSIC are calibrated using a standard solution of potassium hydrogen phthalate (KHP) and sodium carbonate and bicarbonate mixture (Na_2CO_3+$NaHCO_3$), respectively. The MDLs was 4 μg L^{-1} for TWSC/WSIC.

Portions of the quartz filters (0.5 cm^2 punches) were analyzed for organic carbon (OC) and elemental carbon (EC) using a DRI Model 2001 thermal/optical carbon analyzer (Atmoslytic Inc., USA). OC and EC were obtained following the IMPROVE_A protocol (Chow et al., 2007): OC was quantified as the sum of four OC fractions plus a pyrolyzed organic carbon fraction (OP) while EC was measured as the sum of three elemental carbon fractions minus OP. The MDLs for OC and EC were below 0.41 and 0.03 μg cm^{-2}. Replicates were measured one in ten samples and the difference determined was smaller than 10% for OC and EC. QA/QC procedures for these analyses have been described by Cao et al. (2003).

The concentrations of elements were determined by energy dispersive X–ray fluorescence (ED–XRF) spectrometry (Epsilon 5 XRF analyzer, PANalytical, the Netherlands). The analytical details and QA/QC procedures have been described in Zhang et al. (2014c). Teflon™ samples were not collected from November to December, 2011, and therefore, portions of the quartz–fiber filters for that period were used to determine the concentrations of a subset of the elements, including Fe, Pb, S, Cl. Other elements, such as Si, Ca and Al, were not quantified in the quartz–filter samples because blank values were high and variable. The accuracies and precisions of the ED–XRF analyses for both Teflon™ and quartz filters have been reported in previous publications (Cao et al., 2012; Xu et al., 2012).

3. Results

3.1. $PM_{2.5}$ mass concentration

The $PM_{2.5}$ mass loadings ranged from 5.7 to 149.7 μg m^{-3} (Figure 1), and more than 90% of the results were lower than the Target–2 standard for 24–h average $PM_{2.5}$ mass (75 μg m^{-3}) that is a part of the new Ambient Air Quality Standards for China (GB3095–2012). On the other hand, the annual average $PM_{2.5}$ mass (38.9 μg m^{-3}) was slightly higher than Target–2 standard for annual mean $PM_{2.5}$ value of 35 μg m^{-3}. The relative standard deviation of the annual mean $PM_{2.5}$ was 66% (Table 1), and this is indicative of large variability in aerosol loadings caused by extreme events, such as dust storms.

The $PM_{2.5}$ showed the highest seasonal values during spring, followed by winter, and lowest concentrations occurred during summer. The ratio between the spring and summer averages of aerosol mass was 2.38. The trends in $PM_{2.5}$ mass concentrations observed at QHL are similar to the temporal variations in TSP at Waliguan where the mass loadings started to increase in early autumn, reached maximum values in April, then decreased from May to August (Qi et al., 2012). The higher aerosol concentrations in winter and spring could be explained by diminished precipitation as well as the increased influxes of dust brought by strong westerly winds. The three–day trajectories at 500 m a.g.l. were computed by using the NOAA HYSPLIT4 model to support the speculation, and

clusters were determined with the mean trajectory of each cluster in four seasons (see the SM, Figure S2). In spring and winter, air masses transported mainly from the west (Central Asia and Western China) and northwest, accounted for ~80% of the whole trajectories in the two seasons. However, in summer, only 12% air masses transported from the west.

Indeed, four dust storms (DSs) occurred during the year of the measurements. These were in late winter to early spring on 24 February, 19 March, 18 April, and 24 April (see areas shaded in orange in Figure 1). The aerosol mass loadings for these events were 93.9, 83.7, 71.7, and 149.7 μg m^{-3}, respectively, and therefore, the arithmetic mean for the high dust samples was 99.7 μg m^{-3}. This is about 3 times the yearly mean value when the high concentrations for these episodes are excluded. Three–day back trajectories for the dust storm events, calculated for 500, 1 000 and 1 500 m a.g.l., were presented in Figure S3 (see the SM). Trajectories of DS–1, DS–2 and DS–3 episodes were mainly from west (Central Asia and Western China), while air mass of DS–4 was transported faster from the northwest and with a higher planetary boundary layer, which brought the highest level of mass in the whole sampling time. After excluding the data for DS events, the seasonally averaged $PM_{2.5}$ mass concentrations decreased slightly from winter (41.6 μg m^{-3}) to spring (40.3 μg m^{-3}) while larger decreases into autumn (32.2 μg m^{-3}) and summer (22.1 μg m^{-3}). This demonstrates the strong impact of springtime dust storms on the aerosol mass loadings, and previous studies revealed that dust storms do impact aerosol population on high–altitude site (Zhao et al., 2013; Xu et al., 2014). In addition, an increase of coal and yak–dung burning during the heating season likely also contributed to the relatively high $PM_{2.5}$ concentrations. Likely causes for the lower aerosol concentrations during summer may ascribe to the removal of particles by wet scavenging and the suppression of dust by increased vegetative cover following the spring greening.

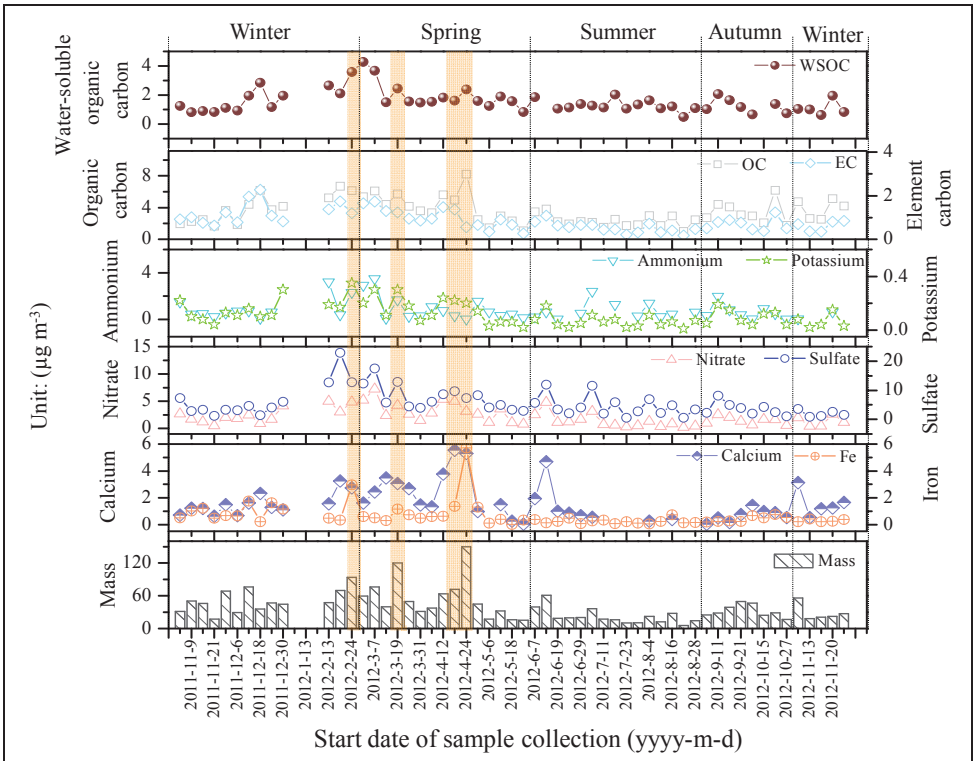

Figure 1. *Temporal variations of chemical species in $PM_{2.5}$ from Qinghai Lake (November 2011 to November 2012).*

Table 1. *$PM_{2.5}$ mass and chemical composition at Qinghai Lake. Units: μg m^{-3}*

Analyte	Spring (15) [a]	Summer (15)	Autumn (8)	Winter (18)	Annual (56)
Mass	52.56±34.64 [b]	22.05±14.30	32.16±11.46	44.47±21.87	38.87±25.83
Organic carbon (OC)	4.13±1.93	2.31±0.75	3.41±1.43	3.88±1.60	3.46±1.64
Elemental carbon (EC)	1.00±0.45	0.53±0.24	0.69±0.29	1.05±0.52	0.84±0.46
OC/EC	4.52±2.82	4.78±1.48	4.98±0.91	4.15±1.81	4.54±1.95
Water–soluble OC	1.96±0.92	1.27±0.38	1.24±0.50	1.53±0.84	1.55±0.77
SO_4^{2-}	7.49±4.16	4.54±3.47	3.65±2.23	5.31±5.64	5.45±4.45
NO_3^-	3.25±1.86	1.32±1.28	1.42±0.67	2.15±1.40	2.12±1.60
Ca^{2+}	2.39±1.70	1.29±1.46	0.66±0.45	1.53±0.83	1.60±1.32
NH_4^+	0.93±1.06	0.73±0.70	0.62±0.63	0.85±0.90	0.81±0.86
K^+	0.15±0.09	0.06±0.04	0.10±0.06	0.13±0.09	0.11±0.08
Mg^{2+}	0.18±0.11	0.07±0.08	0.10±0.03	0.14±0.09	0.12±0.10
Na^+	0.99±0.61	0.51±0.46	0.26±0.14	1.06±1.97	0.79±1.21
Cl^-	0.91±0.64	0.46±0.35	0.46±0.13	0.65±0.67	0.64±0.56

[a] *Number of samples in parentheses*
[b] *Arithmetic mean±standard deviation*

3.2. Chemical compositions

Carbonaceous aerosol. Table 1 also provides summary statistics for water–soluble ions, OC, and EC in $PM_{2.5}$. The yearly average values of OC and EC were 3.5 and 0.8 μg m^{-3}, respectively; these accounted for 9.0% and 2.2% of $PM_{2.5}$ mass. Previous studies have pointed out that EC/TC ratios range from 0.6 to 0.7 in fuel combustion emissions and from 0.1 to 0.2 in biomass combustion emissions (Salam et al., 2003) The EC/TC ratio in our QHL was 0.20±0.05, suggesting that carbonaceous aerosol may be influenced by biomass burning. The mass concentrations of OC and EC showed pronounced seasonal variability with low concentrations of both in summer presumably due to the wash–out of aerosols, and relatively high concentrations in spring and winter likely a result of domestic heating emissions (Figure 2). The seasonal mean OC/EC ratios were essentially the same (4.5±2.8, 4.8±1.5, 5.0±0.9 and 4.1±1.8 for spring, summer, autumn and winter, respectively). This suggests that the combustion sources for the carbonaceous particles are relatively simple and stable throughout the year, and this value is possibly representative of carbonaceous aerosol over a regional scale.

The WSOC concentrations ranged from 0.5 to 4.3 μg m^{-3} in the whole sampling time (average: 1.6±0.8 μg m^{-3}), accounting for 47.8±16.2% of OC, which is higher than what has been observed at urban locations (Ho et al., 2006; Ram and Sarin, 2010), but similar to values at remote sites, such as Manora Peak, India (Ram and Sarin, 2010) and Sapporo, Japan (Aggarwal and Kawamura, 2009). High percentages (>40%) of WSOC in OC have been reported for aged aerosols (Jaffrezo et al., 2005), as well as for biomass burning aerosols (Kundu et al., 2010; Shen et al., 2014a). A biomass burning source for OC and WSOC at QHL can be inferred from the significant linear correlations between OC and K^+ (r=0.70) and WSOC and K^+ (r=0.72) (see the SM, Figure S4a) because K^+ is generally acknowledged to be enriched in biomass burning aerosols (Shen et al., 2009). Moreover, similar correlations also were found between SO_4^{2-} and NO_3^- versus WSOC (r=0.68, r=0.77, Figure S4b), and this suggests a contribution of SOA to WSOC because SO_4^{2-} can promote the formation SOA (Szmigielski et al., 2010).

WSOC concentrations decreased in the order spring (2.0± 0.9 μg m^{-3})>winter (1.5±0.8 μg m^{-3})>summer (1.3±0.4 μg m^{-3})> autumn (1.2±0.5 μg m^{-3}). Greater emissions from biomass burned for heating, especially yak dung, is a likely reason for the higher WSOC during the colder seasons. In addition, after excluding the data for the samples collected during the DS events, WSOC exhibited slightly higher correlations with EC in spring and winter (r=0.80 and r=0.77 respectively) compared with summer and autumn (r=0.59 and r=0.61 respectively, see the SM, Figure S5). This is further evidence that biomass burning has a greater influence on the aerosol populations during spring and winter compared with the other two seasons.

Water–soluble ions. Of the water–soluble ions analyzed, it accounted for 29.7% the total $PM_{2.5}$. SO_4^{2-} ranked highest in terms of mass, while the relative abundances of the other ions followed the order NO_3^->Ca^{2+}>NH_4^+>Na^+>Cl^->K^+>Mg^{2+}. The combined concentrations of SO_4^{2-}, NO_3^-, and NH_4^+, all of which can form as secondary inorganic aerosols, accounted for the majority (72.5%) of the total measured ion mass. The arithmetic mean sums of the concentrations of the eight ions analyzed were 16.1, 8.2, 7.3 and 11.6 μg m^{-3} in spring, summer, autumn and winter, respectively; and these amounted to 32.9%, 34.4%, 24.0%, and 25.5% of the total $PM_{2.5}$ mass. The seasonal variations of five ions (SO_4^{2-}, NO_3^-, NH_4^+, K^+ and Ca^{2+}) are presented in Figure 1. SO_4^{2-}, NO_3^-, NH_4^+ and K^+ showed clear seasonality with peaks in the concentrations of in late winter and early spring, and lower concentrations in summer and autumn. Major peaks in OC, EC, and WSOC always coincided with high loadings of these same four major inorganic ions, and this implies that combustion sources and possibly removal processes caused these species' concentrations to co–vary. Seasonal variations were particularly pronounced for Ca^{2+}, showed a nearly 4–fold increase from autumn (0.7±0.5 μg m^{-3}) to spring (2.4± 1.7 μg m^{-3}). The high springtime concentrations can be explained by the more frequent occurrences of dust events compared the other seasons. The concentrations of the five ions in winter and spring also were more variable than those in summer and autumn, implying rather complex sources for these species in winter and spring.

Ion balance calculations are useful to evaluate the acid–base balance of particulate matter, which could be seen in previous studies (Qu et al., 2008; Shen et al., 2009; Shen et al., 2014b). The charge balance between the total cations (Σ^+) and total anions (Σ^-) (including dust storm data) is shown in Figure S6a (see the SM). Strong correlations between the two totals indicates most of the ionic components were measured, and the fact that the average Σ^+/Σ^- ratio is less than unity throughout the year implies that the $PM_{2.5}$ aerosols were slightly acidic.

A scatter plot between the equivalent concentrations of NH_4^+ and SO_4^{2-} at QHL is shown in Figure S6b, and the 0.5:1 and 1:1 equivalence lines, which represent the proportions of the two ions in ammonium sulfate [$(NH_4)_2SO_4$] and ammonium bisulfate [NH_4HSO_4], respectively, also are shown. A good correlation between NH_4^+ and SO_4^{2-} and the fact that the NH_4^+/SO_4^{2-} equivalent ratio varies from 0.01 to 0.68 (average: 0.32±0.20), suggested the relatively low concentrations of NH_3 in background air over the TP lead to the formation of ammonium sulfate [$(NH_4)_2SO_4$].

To further investigate the relationships among the aerosol ions, we examined the correlations between [NH_4^++Ca^{2+}] and [SO_4^{2-}] (see the SM, Figure S6c) and [NH_4^++Ca^{2+}+Mg^{2+}] and [SO_4^{2-}] (Figure S6d). The ions were strongly correlated throughout the year, with correlation coefficients significant at p<0.0001, and slopes of regression lines approaching unity, indicating the existence of $CaSO_4$ and $MgSO_4$ in addition to $(NH_4)_2SO_4$. The relatively low concentrations of NH_4^+ compared with more impacted areas suggests that water–soluble Ca^{2+} from mineral dust is important for the neutralization of acidic species at our remote site (Shen et al., 2008).

Comparison with literature reports. A comparison of the mass and chemical compositions measured at different locations is given in Table S1 (see the SM). The mean concentration for summer $PM_{2.5}$ samples (21.27 μg m^{-3}) in QHL reported by Zhang et al. (2014a) was similar to the value as we measured (22.05 μg m^{-3}), and the chemical differences of these two studies are also not too much. Besides the sampling periods difference, the samplers using in these two studies are also different. In the campaign of 2010, high flow rate (1.0 m^3 min^{-1}) and long sampling time (120 h) were conducted during samples collection in comparison with low volume sampler here. In this study, a mean ratio of $PM_{2.5}$ TSP^{-1} ratio at QHL in summer is 0.51, so a rough estimate of TSP concentration (~79.8 μg m^{-3}) can be included here for comparison. As expected, the aerosol mass values observed at our Bird Island station were much lower than urban areas, such as Beijing (Zhang et al., 2013) and Xi'an (Zhang et al., 2011), and also lower than PM_{10} levels in Xining (Xining EPA, 2012) or Lhasa (Zhang et al., 2012a), the provincial capital of Qinghai and Tibet, and this shows that QHL is much less affected by anthropogenic sources than those cities. Further comparisons show that the estimated average TSP at QHL is similar to values at Manora Peak (Central Himalayas, 69.38 μg m^{-3}) and Mt. Waliguan (76 μg m^{-3}) for November 2002 to August 2009 (Ram et al., 2010; Qi et al., 2012). The relatively low aerosol mass at QHL is the first indication that the site may be

representative of background conditions in the interior of Eurasia. Any increases from the low background concentrations might reflect some extra input from both natural and human activities.

However, QHL $PM_{2.5}$ and the estimated TSP mass concentrations were significantly higher than those in some remote sites: four times higher than QSS station (9.49 μg m^{-3} in $PM_{2.5}$, 4 180 m a.s.l, Northern boundary of TP) (Xu et al., 2014); approximately three to ten times higher than at Lulang (23.49 μg m^{-3} in TSP, 3 360 m a.s.l., Southeast TP) (Zhao et al., 2013), Nam Co (7 μg m^{-3} in TSP, 4 730 m a.s.l, Central of TP) (Cong et al., 2009), NCO–P site (3.82 μg m^{-3} in PM_{10}, 5 079 m a.s.l., Southern Himalayas) (Marinoni et al., 2010) and one order of magnitude higher than Jungfraujoch (3 580 m a.s.l., Swiss Alps) (Cozic et al., 2008). For the chemical compositions, in general, OC, EC and ion concentrations at QHL were much lower than those in urban areas. The comparison with the data at high–altitude sites shows that the concentrations of most compositions at QHL are 2–10 times higher than those at TP or continental background sites, such as Lulang (Zhao et al., 2013), NCO–P (Decesari et al., 2010) , QOMS (Cong et al., 2014), QSS (Xu et al., 2014), Mt. Fuji (Suzuki et al., 2008), Jungfraujoch (Krivacsy et al., 2001), Mt. Sonnblick, Puy de Dome and Schauinsland (Pio et al., 2007) excepet Monora Peak. The relatively higher concentration of chemical compositions in Monora Peak could be ascribed to the influence by fossil fuel and biomass burning emissions from the South Asian Sub–Continent (Ram et al., 2010). This comparison also shows that the carbonaceous aerosol and major ions at QHL were influenced by anthropogenic sources even though is a remote site.

Coefficients of divergence for different seasons. The coefficient of divergence (CD), a self–normalizing parameter, was used to evaluate the differences in the average concentrations of major chemical species at the QHL site for paired seasons. The CD is calculated as:

$$CD_{jk} = \sqrt{\frac{1}{p}\sum_{i=1}^{p}\left(\frac{x_{ij}-x_{ik}}{x_{ij}+x_{ik}}\right)^2} \quad (1)$$

where, j and k stand for the two seasons being compared, p is the number of components investigated, and x_{ij} and x_{ik} represent the average mass concentrations of chemical component i during seasons j and k. Here the data for pairs of seasons were compared after excluding all dust episodes. A low CD (approaching zero) and a high correlation coefficient are expected for seasons and sites impacted by similar particulate matter sources.

Overall, the CD values for the pairs of seasons ranged from 0.17 to 0.28, together with high correlation coefficients (r^2>0.98) in all paired season (see the SM, Figure S7), and this indicates that the seasonal changes in chemical composition were relatively modest. Nevertheless, the CDs for winter versus spring (0.17) and autumn versus summer (0.19) were lower than others, and this suggests some season–to–season variability in the chemistry of the aerosol followed by the other paired seasons. Moreover, the data for the water–soluble ions (Na^+, Cl^-, Ca^{2+}, SO_4^{2-} and NO_3^-) plotted further from the 1:1 line than OC and EC in the winter/spring and autumn/summer pairs, and this shows that the differences in ions were larger than carbonaceous aerosols.

3.3. Yak dung burning versus ambient aerosol samples

Chemical profiles of yak dung burning sample. We analyzed $PM_{2.5}$ yak dung burning sample collected from the local residential area to determine whether those emissions are an important source for the carbonaceous or ionic components of the aerosol. The concentrations of selected chemical components of the yak–dung burning samples are shown in Figure 2. The carbonaceous fraction is dominant in terms of the $PM_{2.5}$ mass, with concentrations of 5 868.90 and 213.42 μg per filter for OC and EC, respectively. The OC/EC ratio was 27.50 for yak–dung burning, and this is much higher than the ratios for biomass burning (6.6) (Saarikoski et al., 2008), wood burning (4.2, 10.7) or coal combustion (2.7, 7.6) (Watson et al., 2001; Zhang et al., 2012b). The relative abundances of the OC and EC are known to differ among carbon sources (Chow et al., 2004). In the yak dung–burning samples, OC2 was the main component of TC (36.4%), and the second most abundant component was OC1 (32.0%). In comparison, the measured EC fractions contributed only small percentages (3.5%) of the TC. These results are somewhat similar to what has been found for burning straw samples. For example, Cao et al. (2005) reported that OC1 was the main component (36.8%) of TC from straw–burning, and it was followed by OC2 (29.2%) while EC1 only made up 0.4% of the TC.

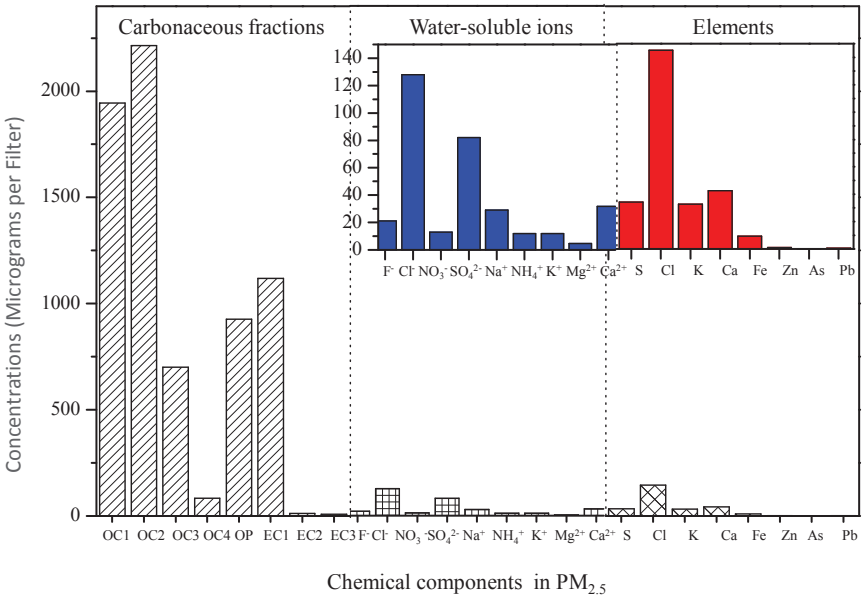

Figure 2. *Concentrations of selected chemical components in burning yak–dung sample.*

The sums of the concentrations of the eight ions in the yak dung–burning sample were 332.98 μg per filter, which is roughly 5 to 6% of the carbonaceous aerosol. Of the water soluble ions, Cl^- and SO_4^{2-} were the most abundant in the burnt dung samples, accounting for 38.43% and 24.64% of the measured ion mass, respectively. With reference to the elemental data, Cl is the most abundant fraction, and it was followed by Ca, S and K. The levels for these four elements are comparable with those of the water soluble ions.

Comparision of chemical profiles between ambient and source samples. The average percentages of eight fractions in ambient (excluding dust episodes) samples are shown in Figure S8a (see the SM). The annual average abundances of OC1, OC2, OC3, OC4, EC1–OP, EC2, EC3 and OP in TC were 4.7%, 14.3%, 26.3%, 21.3%, 15.3%, 3.9%, 0.4% and 14.1%, respectively. The contributions of OC3, OC4 and EC1–OP in the ambient samples were much higher (~2.3, 10.2 and 4.8) than those in yak dung–burning samples, suggesting that the carbonaceous aerosol in the QHL region is influenced by fossil fuel combustion, most likely coal burning, in addition to yak–dung burning.

The seasonal variations in the carbon fractions at QHL were different from what has been observed in urban areas, including Xi'an and several cities in the Pearl River Delta Region. The seasonality was, however, somewhat similar to results from Hok Tsui, a rural site in Hong Kong, which has relatively high abundances of OC2 and OC3 (Cao et al., 2004). At both QHL and Hok Tsui these two OC fractions increase from winter to summer. Higher temperatures and more intense solar radiation during the summer months provide conditions favorable for photochemical activity and SOC production (Shen et al., 2014b), and this may explain the seasonality in OC2 and OC3, at least in part. Further comparisons show that the impact from motor vehicles at QHL is likely less than at Hok Tsui because the abundances of EC2 and EC3 at QHL were relatively low.

The relative proportions of the water–soluble ions in the ambient aerosol differed from those in the yak dung–burning samples. That is, the $PM_{2.5}$ showed lower abundances of Cl^- and K^+ and higher percentages of NH_4^+, NO_3^- and SO_4^{2-} compared with the yak–dung burning samples (Figure S8b). This is evidence that the water–soluble ions in the $PM_{2.5}$ were mainly secondary pollutants and not strongly impacted by the burning of yak dung. To further test this conclusion, we calculated and compared SO_4^{2-}/OC ratios in the $PM_{2.5}$ and emission samples. This ratio was found to be informative, because the ratios for the burnt yak–dung samples was 0.014, at that was far lower than what was observed in the ambient samples (range: 0.2~5.4, average: 1.6±1.0). This large difference supports the conclusion that the composition of the ambient aerosols was not greatly impacted by yak–dung burning but rather by other sources, especially fossil fuel combustion.

3.4. Material balance

The relative contributions of major chemical species to $PM_{2.5}$ mass for different seasons are shown in Figure S9 (see the SM). Organic matter (OM) were calculated as twice the OC content–the conversion factor is slightly higher than that for urban areas (e.g. OM=1.2~1.6×OC) (Turpin and Lim, 2001) because of the aging of aerosols during transport and other factors have been shown to result in a greater proportion of oxygenated organic aerosols relative to hydrocarbon–like organic aerosols at a remote site. Iron often has been used a marker for fugitive dust, and we assumed an Fe of 4% in crustal material to estimate the loadings of mineral dust (Zhang et al., 2003).

$$\text{Mineral dust}=\text{Fe}/4\% \quad (2)$$

Given that the sampling site is ~1 km away from Qinghai Lake, we considered chloride salts as a probable component of $PM_{2.5}$ population, so it was included in our evaluation of material balance from the following equation:

$$\text{Salt}=Cl^-+1.4486\times Na^+ \quad (3)$$

in which 1.4486 is the ratio of the sum concentrations of all elements except Cl^- in sea water divided by the concentration of Na^+ (Li et al., 2010). Following the approach of Landis et al. (2001) , we estimated the combined contributions of the trace element oxides (TEO) from the following equation:

$$\text{TEO}=1.3\times[0.5\times(\text{Sr+Ba+Mn+Co+Rb+Ni+V})+1.0\times(\text{Cu+Zn+Mo+Cd+Sn+Sb+Tl+Pb+As+Se+Ge+Cs+Ga})] \quad (4)$$

The combined masses reconstructed as described above accounted for 90.8, 88.6, 78.1, and 90.5% of measured $PM_{2.5}$ mass in spring, summer, autumn and winter, respectively. Mineral dust was the dominant $PM_{2.5}$ species in all seasons, and it was followed by OM and SO_4^{2-}, with some variability in the percentages of dust in the four seasons but an average of ~40% to the $PM_{2.5}$ mass overall. It has been similarly shown that the aerosol particles at the Waliguan Observatory were predominantly from natural sources, mainly soil particles and weathered crustal material (Gao and Anderson, 2001; Wen et al., 2001). In spring and winter, mineral dust made up about half of the $PM_{2.5}$ mass at QHL. In summer, the percentages of OM and SO_4^{2-} increased while mineral dust decreased by ~40% compared with the spring. Indeed, the secondary aerosol species (SO_4^{2-}, NO_3^- and NH_4^+) combined to account for ~30% of the measured mass in summer, suggesting an increasingly important role for these substances in the warmer part of the year. In autumn, the mineral dust increased slightly over summer, but it was still lower than in spring or winter.

When the dataset was restricted to typical conditions, that is, dust storm events were excluded, the average percentages of OM, EC, K^+, NH_4^+, NO_3^- and mineral dust relative to the total $PM_{2.5}$ mass showed comparatively small differences among the four seasons (see the SM, Table S2), though different monsoons dominated in different seasons (e.g. westerlies dominated in winter and spring while East Asia monsoon dominated in summer). Therefore, there are several important implications for this finding: first that natural sources (Mineral dust to mass: 30%~40%) play a dominant role in aerosol particles and the $PM_{2.5}$ sources in QHL are relatively stable. Second, natural sources have significant impact on the sampling site relative to anthropogenic sources. Finally, under typical conditions, the chemical composition of $PM_{2.5}$ from the QHL region may be representative of the larger regional characteristics of particulate matter.

4. Conclusions

$PM_{2.5}$ samples were collected at the QHL Observatory on the northeastern edge of the TP from 2011–2012. The grand average $PM_{2.5}$ mass concentration was 38.9±25.8 μg m^{-3} (range: 5.7 to 149.7 μg m^{-3}), and this can be considered representative of background conditions over inland Eurasia. The yearly average values of OC, EC, water–soluble ions were 3.5, 0.8, and 11.3 μg m^{-3}, respectively, and these accounted for 9.0%, 2.2% and 29.7% of $PM_{2.5}$ mass. The $PM_{2.5}$ mass and all of the chemical substances measured (OC, EC, WSOC, SO_4^{2-}, NO_3^-, NH_4^+ and K^+) showed higher values in spring and winter compared with summer, and this was likely caused by greater combustion emissions during the heating season and more wet scavenging of the aerosol in summer.

Investigations into the sources for the carbonaceous ionic fractions in the ambient samples indicate that coal combustion residues were present along with those from local yak–dung burning. Material balance analyses showed that mineral dust was

the most abundant species at this background site in terms of mass, contributing ~40% to the $PM_{2.5}$ mass. Perturbations from local human sources were clearly evident at this site despite its remoteness. After excluding the data for dust events, the percentages of OM, EC, K^+, NH_4^+, NO_3^- and mineral dust showed little difference among the four seasons. This implies that the many of the anthropogenic sources that affect the atmosphere at QHL are relatively stable and that the $PM_{2.5}$ from the region may reflect the regional characteristics of particulate matter. The results from this site provide valuable insights into chemical characteristics of particles in the middle troposphere over a remote continental region, and the data should be useful for models studies of long–range pollution transport and climate change.

Acknowledgment

This work was financially supported by the Ministry of Science & Technology of China (2007BAC30B00, 2012BAH31B00).

Supporting Material Available

Location of the sampling site (a and b) and (c) picture of the sampling tower (Figure S1), Cluster analysis of the three–day air mass back trajectories at QHL during the sampling periods by using the HYSPLIT model (Figure S2), Three–day air backward–in–time air mass trajectory analysis for dust storm episodes at QHL (Figure S3), Linear regressions for $PM_{2.5}$: (a) organic carbon (OC) and water–soluble organic carbon (WSOC) versus K^+, (b) WSOC versus NO_3^- and SO_4^{2-} (Figure S4), Linear regressions for water–soluble organic carbon (WSOC) versus elemental carbon (EC) in four seasons (Figure S5), Relationships between selected cations and anions: (a) total cations versus total anions, (b) $[NH_4^+]$ versus $[SO_4^{2-}]$, (c) $[NH_4^+ + Ca^{2+}]$ versus $[SO_4^{2-}]$, (d) $[NH_4^+ + Ca^{2+} + Mg^{2+}]$ versus $[SO_4^{2-}]$ (Figure S6), Coefficients of divergence (CD) between two seasons for the average concentrations of chemical species in $PM_{2.5}$ (Figure S7), Abundances in ambient and source samples of (a) eight thermally–defined carbon fractions and (b) eight water–soluble ions (Figure S8), Pie charts showing re–constructed chemical composition for $PM_{2.5}$ from the Qinghai Lake region (Figure S9), Comparison of $PM_{2.5}$ mass, OC, EC, ions at Qinghai Lake with other high–altitude background sites worldwide and four cities in China (Table S1), Percentages of selected chemical components in total mass on normal days (dust storm events excluded) (Table S2). This information is available free of charge via the Internet at http://www.atmospolres.com.

References

Aggarwal, S.G., Kawamura, K., 2009. Carbonaceous and inorganic composition in long–range transported aerosols over Northern Japan: Implication for aging of water–soluble organic fraction. *Atmospheric Environment* 43, 2532–2540.

Cao, J.J., Shen, Z.X., Chow, J.C., Watson, J.G., Lee, S.C., Tie, X.X., Ho, K.F., Wang, G.H., Han, Y.M., 2012. Winter and summer $PM_{2.5}$ chemical compositions in fourteen Chinese cities. *Journal of the Air & Waste Management Association* 62, 1214–1226.

Cao, J.J., Wu, F., Chow, J.C., Lee, S.C., Li, Y., Chen, S.W., An, Z.S., Fung, K.K., Watson, J.G., Zhu, C.S., Liu, S.X., 2005. Characterization and source apportionment of atmospheric organic and elemental carbon during fall and winter of 2003 in Xi'an, China. *Atmospheric Chemistry and Physics* 5, 3127–3137.

Cao, J.J., Lee, S.C., Ho, K.F., Zou, S.C., Fung, K., Li, Y., Watson, J.G., Chow, J.C., 2004. Spatial and seasonal variations of atmospheric organic carbon and elemental carbon in Pearl River Delta Region, China. *Atmospheric Environment* 38, 4447–4456.

Cao, J.J., Lee, S.C., Ho, K.F., Zhang, X.Y., Zou, S.C., Fung, K., Chow, J.C., Watson, J.G., 2003. Characteristics of carbonaceous aerosol in Pearl River Delta Region, China during 2001 winter period. *Atmospheric Environment* 37, 1451–1460.

Chow, J.C., Watson, J.G., Chen, L.W.A., Chang, M.C.O., Robinson, N.F., Trimble, D., Kohl, S., 2007. The IMPROVE_A temperature protocol for thermal/optical carbon analysis: Maintaining consistency with a long–term database. *Journal of the Air & Waste Management Association* 57, 1014–1023.

Chow, J.C., Watson, J.G., Kuhns, H., Etyemezian, V., Lowenthal, D.H., Crow, D., Kohl, S.D., Engelbrecht, J.P., Green, M.C., 2004. Source profiles for industrial, mobile, and area sources in the big bend regional aerosol visibility and observational study. *Chemosphere* 54, 185–208.

Cong, Z., Kang, S., Kawamura, K., Liu, B., Wan, X., Wang, Z., Gao, S., Fu, P., 2014. Carbonaceous aerosols on the south edge of the Tibetan Plateau: concentrations, seasonality and sources. *Atmospheric Chemistry and Physics Discussions* 14, 25051–25082.

Cong, Z.Y., Kang, S.C., Smirnov, A., Holben, B., 2009. Aerosol optical properties at Nam Co, a remote site in central Tibetan Plateau. *Atmospheric Research* 92, 42–48.

Cozic, J., Verheggen, B., Weingartner, E., Crosier, J., Bower, K.N., Flynn, M., Coe, H., Henning, S., Steinbacher, M., Henne, S., Coen, M.C., Petzold, A., Baltensperger, U., 2008. Chemical composition of free tropospheric aerosol for PM_1 and coarse mode at the high alpine site Jungfraujoch. *Atmospheric Chemistry and Physics* 8, 407–423.

Decesari, S., Facchini, M.C., Carbone, C., Giulianelli, L., Rinaldi, M., Finessi, E., Fuzzi, S., Marinoni, A., Cristofanelli, P., Duchi, R., Bonasoni, P., Vuillermoz, E., Cozic, J., Jaffrezo, J.L., Laj, P., 2010. Chemical composition of PM_{10} and PM_1 at the high–altitude Himalayan station Nepal Climate Observatory–Pyramid (NCO–P) (5 079 m a.s.l.). *Atmospheric Chemistry and Physics* 10, 4583–4596.

Engling, G., Zhang, Y.N., Chan, C.Y., Sang, X.F., Lin, M., Ho, K.F., Li, Y.S., Lin, C.Y., Lee, J.J., 2011. Characterization and sources of aerosol particles over the Southeastern Tibetan Plateau during the Southeast Asia biomass–burning season. *Tellus Series B–Chemical and Physical Meteorology* 63, 117–128.

Gao, Y., Anderson, J.R., 2001. Characteristics of Chinese aerosols determined by individual–particle analysis. *Journal of Geophysical Research–Atmospheres* 106, 18037–18045.

Ho, K.F., Lee, S.C., Cao, J.J., Li, Y.S., Chow, J.C., Watson, J.G., Fung, K., 2006. Variability of organic and elemental carbon, water soluble organic carbon, and isotopes in Hong Kong. *Atmospheric Chemistry and Physics* 6, 4569–4576.

Jaffrezo, J.L., Aymoz, G., Delaval, C., Cozic, J., 2005. Seasonal variations of the water soluble organic carbon mass fraction of aerosol in two valleys of the French Alps. *Atmospheric Chemistry and Physics* 5, 2809–2821.

Jin, Z.D., Han, Y.M., Chen, L., 2010a. Past atmospheric Pb deposition in Lake Qinghai, Northeastern Tibetan Plateau. *Journal of Paleolimnology* 43, 551–563.

Jin, Z.D., You, C.F., Wang, Y., Shi, Y.W., 2010b. Hydrological and solute budgets of Lake Qinghai, the largest lake on the Tibetan Plateau. *Quaternary International* 218, 151–156.

Krivacsy, Z., Hoffer, A., Sarvari, Z., Temesi, D., Baltensperger, U., Nyeki, S., Weingartner, E., Kleefeld, S., Jennings, S.G., 2001. Role of organic and black carbon in the chemical composition of atmospheric aerosol at European background sites. *Atmospheric Environment* 35, 6231–6244.

Kundu, S., Kawamura, K., Andreae, T.W., Hoffer, A., Andreae, M.O., 2010. Molecular distributions of dicarboxylic acids, ketocarboxylic acids and alpha–dicarbonyls in biomass burning aerosols: Implications for photochemical production and degradation in smoke layers. *Atmospheric Chemistry and Physics* 10, 2209–2225.

Landis, M.S., Norris, G.A., Williams, R.W., Weinstein, J.P., 2001. Personal exposures to $PM_{2.5}$ mass and trace elements in Baltimore, MD, USA. *Atmospheric Environment* 35, 6511–6524.

Lau, K.M., Kim, K.M., 2006. Observational relationships between aerosol and Asian monsoon rainfall, and circulation. *Geophysical Research Letters* 33, art. no. L21810.

Lau, W.K.M., Kim, M.K., Kim, K.M., Lee, W.S., 2010. Enhanced surface warming and accelerated snow melt in the Himalayas and Tibetan Plateau induced by absorbing aerosols. *Environmental Research Letters* 5, art. no. 025204.

Li, J.J., Wang, G.H., Wang, X.M., Cao, J.J., Sun, T., Cheng, C.L., Meng, J.J., Hu, T.F., Liu, S.X., 2013. Abundance, composition and source of atmospheric $PM_{2.5}$ at a remote site in the Tibetan Plateau, China. *Tellus Series B–Chemical and Physical Meteorology* 65, art. no. 20281.

Li, L., Wang, W., Feng, J.L., Zhang, D.P., Li, H.J., Gu, Z.P., Wang, B.J., Sheng, G.Y., Fu, J.M., 2010. Composition, source, mass closure of $PM_{2.5}$ aerosols for four forests in Eastern China. *Journal of Environmental Sciences–China* 22, 405–412.

Marinoni, A., Cristofanelli, P., Laj, P., Duchi, R., Calzolari, F., Decesari, S., Sellegri, K., Vuillermoz, E., Verza, G.P., Villani, P., Bonasoni, P., 2010. Aerosol mass and black carbon concentrations, a two year record at NCO–P (5079 m, Southern Himalayas). *Atmospheric Chemistry and Physics* 10, 8551–8562.

Ministry of Environmental Protection of the People's Republic of China, 2012. *National Ambient Air Quality Standards* (GB3095-2012).

Pio, C.A., Legrand, M., Oliveira, T., Afonso, J., Santos, C., Caseiro, A., Fialho, P., Barata, F., Puxbaum, H., Sanchez–Ochoa, A., Kasper–Giebl, A., Gelencser, A., Preunkert, S., Schock, M., 2007. Climatology of aerosol composition (organic versus inorganic) at nonurban sites on a west–east transect across Europe. *Journal of Geophysical Research–Atmospheres* 112, art. no. D23S02.

Qi, D.–L., Li, X.–D., Cai, Y.–X., Xiao, H.–B., Wang, L., Huang, J.–Q., Li, D.–L., Wang, J.–Q., Liu, P., 2012. Study on distribution characteristics and impact factors of TSP in Qinghai–Tibet Plateau. *China Environmental Science* 32, 2174–2183.

Qu, W.J., Zhang, X.Y., Arimoto, R., Wang, Y.Q., Wang, D., Sheng, L.F., Fu, G., 2009. Aerosol background at two remote CAWNET sites in Western China. *Science of the Total Environment* 407, 3518–3529.

Qu, W.J., Zhang, X.Y., Arimoto, R., Wang, D., Wang, Y.Q., Yan, L.W., Li, Y., 2008. Chemical composition of the background aerosol at two sites in Southwestern and Northwestern China: Potential influences of regional transport. *Tellus Series B–Chemical and Physical Meteorology* 60, 657–673.

Ram, K., Sarin, M.M., 2010. Spatio–temporal variability in atmospheric abundances of EC, OC and WSOC over Northern India. *Journal of Aerosol Science* 41, 88–98.

Ram, K., Sarin, M.M., Hegde, P., 2010. Long–term record of aerosol optical properties and chemical composition from a high–altitude site (Manora Peak) in Central Himalaya. *Atmospheric Chemistry and Physics* 10, 11791–11803.

Ramanathan, V., Carmichael, G., 2008. Global and regional climate changes due to black carbon. *Nature Geoscience* 1, 221–227.

Saarikoski, S., Timonen, H., Saarnio, K., Aurela, M., Jarvi, L., Keronen, P., Kerminen, V.M., Hillamo, R., 2008. Sources of organic carbon in fine particulate matter in Northern European urban air. *Atmospheric Chemistry and Physics* 8, 6281–6295.

Salam, A., Bauer, H., Kassin, K., Ullah, S.M., Puxbaum, H., 2003. Aerosol chemical characteristics of a mega–city in Southeast Asia (Dhaka–Bangladesh). *Atmospheric Environment* 37, 2517–2528.

Shen, Z.X., Cao, J.J., Zhang, L.M., Liu, L., Zhang, Q., Li, J.J., Han, Y.M., Zhu, C.S., Zhao, Z.Z., Liu, S.X., 2014a. Day–night differences and seasonal variations of chemical species in PM_{10} over Xi'an, Northwest China. *Environmental Science and Pollution Research* 21, 3697–3705.

Shen, Z.X., Cao, J.J., Zhang, L.M., Zhao, Z.Z., Dong, J.G., Wang, L.Q., Wang, Q.Y., Li, G.H., Liu, S.X., Zhang, Q., 2014b. Characteristics of surface O_3 over Qinghai Lake area in Northeast Tibetan Plateau, China. *Science of the Total Environment* 500, 295–301.

Shen, Z.X., Cao, J.J., Arimoto, R., Han, Z.W., Zhang, R.J., Han, Y.M., Liu, S.X., Okuda, T., Nakao, S., Tanaka, S., 2009. Ionic composition of TSP and $PM_{2.5}$ during dust storms and air pollution episodes at Xi'an, China. *Atmospheric Environment* 43, 2911–2918.

Shen, Z.X., Arimoto, R., Cao, J.J., Zhang, R.J., Li, X.X., Du, N., Okuda, T., Nakao, S., Tanaka, S., 2008. Seasonal variations and evidence for the effectiveness of pollution controls on water–soluble inorganic species in total suspended particulates and fine particulate matter from Xi'an, China. *Journal of the Air & Waste Management Association* 58, 1560–1570.

Suzuki, I., Hayashi, K., Igarashi, Y., Takahashi, H., Sawa, Y., Ogura, N., Akagi, T., Dokiya, Y., 2008. Seasonal variation of water–soluble ion species in the atmospheric aerosols at the summit of Mt. Fuji. *Atmospheric Environment* 42, 8027–8035.

Szmigielski, R., Vermeylen, R., Dommen, J., Metzger, A., Maenhaut, W., Baltensperger, U., Claeys, M., 2010. The acid effect in the formation of 2–methyltetrols from the photooxidation of isoprene in the presence of NO_x. *Atmospheric Research* 98, 183–189.

Turpin, B.J., Lim, H.J., 2001. Species contributions to $PM_{2.5}$ mass concentrations: Revisiting common assumptions for estimating organic mass. *Aerosol Science and Technology* 35, 602–610.

Wang, Q.Y., Schwarz, J.P., Cao, J.J., Gao, R.S., Fahey, D.W., Hu, T.F., Huang, R.J., Han, Y.M., Shen, Z.X., 2014. Black carbon aerosol characterization in a remote area of Qinghai–Tibetan Plateau, Western China. *Science of the Total Environment* 479, 151–158.

Watson, J.G., Chow, J.C., Houck, J.E., 2001. $PM_{2.5}$ chemical source profiles for vehicle exhaust, vegetative burning, geological material, and coal burning in Northwestern Colorado during 1995. *Chemosphere* 43, 1141–1151.

Wen, Y., Xu, X., Tang, J., Zhang, X., Zhao, Y., 2001. Enrichment characteristics and origin of atmospheric aerosol elemental at Mt. Waliguan. *Quarterly Journal of Applied Meteorology* 12, 400–408.

Xu, J.Z., Wang, Z.B., Yu, G.M., Qin, X., Ren, J.W., Qin, D., 2014. Characteristics of water soluble ionic species in fine particles from a high altitude site on the northern boundary of Tibetan Plateau: Mixture of mineral dust and anthropogenic aerosol. *Atmospheric Research* 143, 43–56.

Xu, H.M., Cao, J.J., Ho, K.F., Ding, H., Han, Y.M., Wang, G.H., Chow, J.C., Watson, J.G., Khol, S.D., Qiang, J., Li, W.T., 2012. Lead concentrations in fine particulate matter after the phasing out of leaded gasoline in Xi'an, China. *Atmospheric Environment* 46, 217–224.

Xu, B.Q., Cao, J.J., Hansen, J., Yao, T.D., Joswia, D.R., Wang, N.L., Wu, G.J., Wang, M., Zhao, H.B., Yang, W., Liu, X.Q., He, J.Q., 2009. Black soot and the survival of Tibetan glaciers. *Proceedings of the National Academy of Sciences of the United States of America* 106, 22114–22118.

Zhang, N.N., Cao, J.J., Liu, S.X., Zhao, Z.Z., Xu, H.M., Xiao, S., 2014a. Chemical composition and sources of $PM_{2.5}$ and TSP collected at Qinghai Lake during summertime. *Atmospheric Research* 138, 213–222.

Zhang, T., Cao, J.J., Chow, J.C., Shen, Z.X., Ho, K.F., Ho, S.S.H., Liu, S.X., Han, Y.M., Watson, J.G., Wang, G.H., Huang, R.J., 2014b. Characterization and seasonal variations of levoglucosan in fine particulate matter in Xi'an, China. *Journal of the Air & Waste Management Association* 64, 1317–1327.

Zhang, R., Cao, J.J., Tang, Y.R., Arimoto, R., Shen, Z.X., Wu, F., Han, Y.M., Wang, G.H., Zhang, J.Q., Li, G.H., 2014c. Elemental profiles and signatures of fugitive dusts from Chinese deserts. *Science of the Total Environment* 472, 1121–1129.

Zhang, R., Jing, J., Tao, J., Hsu, S.C., Wang, G., Cao, J., Lee, C.S.L., Zhu, L., Chen, Z., Zhao, Y., Shen, Z., 2013. Chemical characterization and source apportionment of $PM_{2.5}$ in Beijing: Seasonal perspective. *Atmospheric Chemistry and Physics* 13, 7053–7074.

Zhang, X.Y., Wang, Y.Q., Niu, T., Zhang, X.C., Gong, S.L., Zhang, Y.M., Sun, J.Y., 2012a. Atmospheric aerosol compositions in China: Spatial/temporal variability, chemical signature, regional haze distribution and comparisons with global aerosols. *Atmospheric Chemistry and Physics* 12, 779–799.

Zhang, H.F., Wang, S.X., Hao, J.M., Wan, L., Jiang, J.K., Zhang, M., Mestl, H.E.S., Alnes, L.W.H., Aunan, K., Mellouki, A.W., 2012b. Chemical and size characterization of particles emitted from the burning of coal and wood in rural households in Guizhou, China. *Atmospheric Environment* 51, 94–99.

Zhang, T., Cao, J.J., Tie, X.X., Shen, Z.X., Liu, S.X., Ding, H., Han, Y.M., Wang, G.H., Ho, K.F., Qiang, J., Li, W.T., 2011. Water–soluble ions in atmospheric aerosols measured in Xi'an, China: Seasonal variations and sources. *Atmospheric Research* 102, 110–119.

Zhang, X.Y., Gong, S.L., Arimoto, R., Shen, Z.X., Mei, F.M., Wang, D., Cheng, Y., 2003. Characterization and temporal variation of Asian dust aerosol from a site in the Northern Chinese deserts. *Journal of Atmospheric Chemistry* 44, 241–257.

Zhao, Z., Cao, J., Shen, Z., Xu, B., Zhu, C., Chen, L.W.A., Su, X., Liu, S., Han, Y., Wang, G., 2013. Aerosol particles at a high-altitude site on the Southeast Tibetan Plateau, China: Implications for pollution transport from south Asia. *Journal of Geophysical Research: Atmospheres* 118, 11360–11375.